ISSN 1061-933X, Colloid Journal, 2019, Vol. 81, No. 1, pp. 28–34. © Pleiades Publishing, Ltd., 2019.
Russian Text © S.I. Grashchenkov, 2019, published in Kolloidnyi Zhurnal, 2019, Vol. 81, No. 1, pp. 42–48.

# The Use of the Finite Element Method for Calculating Thermophoresis Velocity of Two Interacting Large Aerosol Particles

**S. I. Grashchenkov***
*Pskov State University, Pskov, 180000 Russia*
**e-mail: grasi@mail.ru*

Received May 28, 2018

**Abstract**—We have considered the use of the finite element method for calculating the thermophoresis velocity of two solid aerosol particles with allowance for their mutual influence on each other. It has been assumed that the sizes of the particles are much larger than the mean free path of molecules in a gas. The proposed approach has been employed to numerically calculate the thermophoresis velocities of axially symmetric particles moving along their rotation axes. The motion of the following particles has been considered: two spherical particles, a spherical particle and a flattened spheroid, and a spherical particle and a prolate spheroid. The results of the calculations for two spherical particles have been compared with the known data obtained analytically.

**DOI:** 10.1134/S1061933X19010058

## INTRODUCTION

In a medium with nonuniform temperature, aerosol particles are affected by thermophoretic forces, which induce their motion. Particles located at a rather short distance from each other may substantially influence their mutual motion. In real aerosol systems, aerosol particles are most likely to approach each other in pairs [1]. The effect of the interaction between aerosol particles on their thermophoretic motion was, for the first time, investigated in [2]. The motion of two spherical particles with equal radii along the line passing through their centers was considered taking into account temperature jumps and isothermal slip of a gas on their surfaces. The same problem was considered in [3] for particles with different radii. Note that, at present, more complete boundary conditions have been obtained than those used in [2, 3]. A corresponding problem was solved in [4] for particles with equal radii under more generalized boundary conditions comprising effects linear with respect to the Knudsen number. The motion of two spherical aerosol particles with the same radius was considered in [5] taking into account temperature jumps and isothermal slip of a gas on their surfaces at an arbitrary direction of gas temperature gradient specified far from the particles and with allowance for their rotation. An approximate reflection method was used in that work. An exact analytical solution of this problem was obtained in [6] by the method of separation of variables for large particles, i.e., particles the sizes of which were much larger than the mean free path of molecules in a gas. The thermophoretic motion of two large aerosol particles along a line passing through their centers was considered in the same work taking into account the phase transition on their surfaces. The thermophoresis of two large liquid droplets without taking into account the phase transition on their surfaces was studied in [7].

The aforementioned analysis shows that, at present, the thermophoretic motion of two spherical particles has been considered in detail. In practice, the shape of particles may, however, be arbitrary. Therefore, it is of interest to study approaches that make it possible to calculate the thermophoresis velocities for two aerosol particles with arbitrary shapes. In this work, an approach is proposed that enables one to perform numerical analysis of such problems by the finite element method. In the analysis, we shall confine ourselves to the cases in which the particle sizes are much larger than the mean free path of molecules in a gas, while Reynolds number $\mathrm{Re} = \frac{\mathbf{U}l}{\nu}$ and Peclet thermal number $\mathrm{Pe} = \frac{\mathbf{U}l}{\chi}$ may be considered to be equal to zero. Here, $\mathbf{U}$ is the characteristic velocity of particles, $l$ is their characteristic size, $\nu$ is the kinematic viscosity of a gas, and $\chi$ is its thermal diffusivity. Therewith, the particle motion is supposed to be induced by a gas temperature gradient specified at a large distance from the particles. Moreover, we assume that, as is known from some additional considerations, e.g., the considerations of symmetry, particles move without rotation.

## PROBLEM FORMULATION

Under the aforementioned limitations, the distributions of temperatures $T_1$, $T_2$, and $T_e$, respectively, inside the first and second aerosol particles and in their vicinities are described by the Laplace equations [8, 9]

$$\Delta T_1 = 0, \quad \Delta T_2 = 0, \quad \Delta T_e = 0, \tag{1}$$

while the distributions of velocities $\mathbf{u}$ and gas pressures $p$ in the vicinities of the particles obey the Stokes equations

$$\nabla p = \mu \Delta \mathbf{u}, \tag{2}$$

$$\nabla \cdot \mathbf{u} = \mathbf{0}, \tag{3}$$

where $\mu$ is the dynamic viscosity coefficient of the gas. In the reference system related to the gas quiescent at a large distance from the particles, the boundary conditions on the surface of the first particle have the following form [8, 9]:

$$T_e = T_1, \tag{4}$$

$$\kappa_e \mathbf{n}_i \nabla T_e = \kappa_{i1} \mathbf{n}_i \nabla T_1, \tag{5}$$

$$\mathbf{u}\mathbf{n}_i = \mathbf{n}_i \mathbf{U}_1, \tag{6}$$

$$\mathbf{u}\boldsymbol{\tau} = g_1 \boldsymbol{\tau} \nabla T_e + \boldsymbol{\tau} \mathbf{U}_{T1}. \tag{7}$$

Here, $\mathbf{n}_i$ is a normal directed from the surface of an aerosol particle inward it, $\boldsymbol{\tau}$ is an arbitrary unit tangential vector drawn from a considered point of the surface, $\kappa_e$ is the thermal conductivity coefficient of the gas, $\kappa_{i1}$ is the thermal conductivity coefficient of the material of the first particle, $g_1 = K_{ts1}/T_{01}$ , $K_{ts1}$ is the thermal slip coefficient of the gas on the surface of the first particle, $T_{01}$ is the average temperature of the gas at the particle surface, and $\mathbf{U}_{T1}$ is the first phartícle thermophoresis velocity determined from the condition of the zero force applied to the particle from the side of the gas. The boundary conditions on the surface of the second particle are identical:

$$T_e = T_2, \tag{8}$$

$$\kappa_e \mathbf{n}_i \nabla T_e = \kappa_{i2} \mathbf{n}_i \nabla T_2, \tag{9}$$

$$\mathbf{u}\mathbf{n}_i = \mathbf{n}_i \mathbf{U}_{T2}, \tag{10}$$

$$\mathbf{u}\boldsymbol{\tau} = g_2 \boldsymbol{\tau} \nabla T_e + \boldsymbol{\tau} \mathbf{U}_{T2}. \tag{11}$$

Here, $\kappa_{i2}$ is the thermal conductivity coefficient of the second particle, $\mathbf{U}_{T2}$ is the thermophoresis velocity of the second particle, $g_2 = K_{ts2}/T_{02}$, $K_{ts2}$ is the thermal slip coefficient of the gas on the surface of the second particle, and $T_{02}$ is the average temperature of the gas at the surface of the second particle. Note that, when numerical calculations are carried out at equal values of $K_{ts1}$ and $K_{ts2}$, the values of $g_1$ and $g_2$ may also be taken equal, because $T_{01}$ and $T_{02}$ are close to one another. In the finite element method, the distribution of this or that value is always searched for in some finite region, with some boundary conditions being imposed on the boundary of this region. In our case, we propose to specify the temperature distribution at this boundary. Moreover, we assume that the boundary located in the gas is situated at such a distance from the particle that we may, with a required accuracy, believe that, in the vicinity of this boundary, the gas is quiescent and its pressure is constant.

## GENERAL CALCULATION SCHEME

According to the finite element method, the region in which the distribution of any value is sought is divided into a set of subregions. As a result, a computational grid is obtained that is used to generate a set of basic functions employed for the approximation of the desired distribution. Therewith, because of errors concerning the rounding, the obtained distribution fluctuates about some true distribution. During the calculation of the surface integrals of the functions containing these distributions, the effect of the fluctuations is accumulated, and the values of these integrals may be calculated with a substantial error. This leads to the fact that, even at a rather accurate calculation of the gas flow velocity distribution, the forces applied to an aerosol particle that are calculated on the basis of this distribution may be obtained with a rather large error. Therefore, in this work, we propose an approach that enables us to calculate the velocities of the steady motion of particles without the direct calculation of the forces applied to them.

Let us express the velocities of the particles in the following form:

$$\mathbf{U}_{T1} = \mathbf{U}_{11} + \mathbf{U}_{12},$$

$$\mathbf{U}_{T2} = \mathbf{U}_{22} + \mathbf{U}_{21}.$$

Here, $\mathbf{U}_{11}$ and $\mathbf{U}_{21}$ are the components of the velocities of the first and second particles, respectively, with these components being due to the thermal slip of the gas on the surface of the first particle. That is, when calculating these velocities, instead of conditions (6) and (7), the following conditions are used on the surface of the first particle:

$$\mathbf{u}\mathbf{n}_i = \mathbf{n}_i \mathbf{U}_{11}, \tag{12}$$

$$\mathbf{u}\boldsymbol{\tau} = g_1 \boldsymbol{\tau} \nabla T_e + \boldsymbol{\tau} \mathbf{U}_{11}, \tag{13}$$

while, on the surface of the second particle, the following condition are imposed instead of conditions (10) and (11):

$$\mathbf{u}\mathbf{n}_i = \mathbf{n}_i \mathbf{U}_{21}, \tag{14}$$

$$\mathbf{u}\boldsymbol{\tau} = \boldsymbol{\tau} \mathbf{U}_{21}. \tag{15}$$

Analogously, $\mathbf{U}_{22}$ and $\mathbf{U}_{12}$ are the components of the velocities of the second and first particles, respectively, with these components being due to the thermal slip of the gas on the surface of the second particle.

They are calculated using, instead of conditions (6) and (7), the conditions

$$\mathbf{u}\mathbf{n}_\mathrm{i} = \mathbf{n}_\mathrm{i}\mathbf{U}_{12}, \tag{16}$$

$$\mathbf{u}\boldsymbol{\tau} = \boldsymbol{\tau}\mathbf{U}_{12}, \tag{17}$$

while conditions (10) and (11) are replaced by

$$\mathbf{u}\mathbf{n}_\mathrm{i} = \mathbf{n}_\mathrm{i}\mathbf{U}_{22}, \tag{18}$$

$$\mathbf{u}\boldsymbol{\tau} = g_2\boldsymbol{\tau}\nabla T_\mathrm{e} + \boldsymbol{\tau}\mathbf{U}_{22}. \tag{19}$$

Let us consider the calculation scheme for the values of $\mathbf{U}_{11}$ and $\mathbf{U}_{21}$. After the temperature distributions have been determined, we exclude the subregion corresponding to the interior of the first particle, and the velocity distribution in the gas will be calculated on the basis of a newly constructed computational grid. The calculation will be performed in the reference system related to the first particle. In this reference system, boundary conditions (12) and (13) acquire the form of

$$\mathbf{u}\mathbf{n}_\mathrm{i} = \mathbf{0}, \quad \mathbf{u}\boldsymbol{\tau} = g_1\boldsymbol{\tau}\nabla T_\mathrm{e}.$$

They may be rewritten as follows [10]:

$$\mathbf{u} = g_1\left(\nabla T_\mathrm{e} - \left(\mathbf{n}\nabla T_\mathrm{e}\right)\mathbf{n}\right), \tag{20}$$

where $\mathbf{n}$ is a vector external with respect to the calculation region and normal to its boundary. At the external boundary of the calculation region, the condition of gas quiescence in its vicinity is transformed into the condition of a uniform distribution of the gas velocity. Taking into account the constancy of the pressure at the aforementioned boundary (this pressure with no violation of the generality may be taken equal to zero when calculating the velocity distributions); this, in turn, leads to zero components of the viscous stress tensor of the gas at this boundary (see the description of this tensor below). It is this condition that will be used as the boundary one for the boundary under consideration. At the same time, we may believe that the thus-calculated gas velocity at this boundary has an absolute value equal to $\mathbf{U}_{11}$ and a direction opposite to it. In turn,

$$\mathbf{U}_{21} = \mathbf{U}_{11} + \mathbf{U}_{2\mathrm{s}},$$

where $\mathbf{U}_{2\mathrm{s}}$ is the velocity of the second particle relative to the first. Therewith, conditions (14) and (15) are transformed into the condition of the equality between the gas velocity on the second particle surface and particle velocity $\mathbf{U}_{2\mathrm{s}}$. To calculate numerically this velocity, we shall consider the region of the second particle as a region filled with some gas, the viscosity of which is so high that it moves as a whole, i.e., as a solid particle. We shall refer to it as a "pseudogas." Under this approach, Eqs. (2) and (3) are applicable to the regions of both the gas and the pseudogas, provided that $\mu$ is the viscosity of a substance at a considered point, which may be located in both the gas and the pseudogas. In the numerical calculations, we shall just specify the substance viscosity in the region of the pseudogas much higher than that in the region of the gas. On the boundary of the second particle, the condition of the equality between the velocities of this particle and the gas will be met automatically due to the fulfillment of Eq. (3) for continuity at this boundary. The velocity obtained for any point of the pseudogas will be equal to $\mathbf{U}_{2\mathrm{s}}$. Since the gas flow is steady, its momentum remains unchanged, thereby corresponding to the zero force applied to the second particle from the side of the gas. Taking into account that the gas flow is also steady and conditions that do not change the gas momentum have been imposed on the external boundaries other than the surface of the first particle, we come to the conclusion that the first particle also does not change this momentum; hence, the total force of the interaction between the first particle and the gas is equal to zero.

Velocities $\mathbf{U}_{22}$ and $\mathbf{U}_{12}$ are calculated analogously. The only difference is that, in this case, the computational grid is obtained by eliminating the subregion corresponding to the interior of the second particle, the calculation is carried out in the reference system related to this particle, while the region corresponding to the first particle is considered as a region filled with the pseudogas.

## CALCULATION OF THERMOPHORESIS VELOCITIES OF AEROSOL PARTICLES USING A WEAK FORM OF PROBLEM FORMULATION

Now, let us describe the scheme for calculating desired distributions of temperatures and velocities by the finite element method. This scheme is similar to that described in [10]; therefore, some features that may be found in the cited work will be omitted. At present, several computer programs are available that allow one to solve numerically the initial set of differential equations by the finite element method using a weak form of the formulation of this set. It is natural that the obtained expressions are desirable to be represented in a form convenient for using in an applied program. In this work, the calculations are performed using the freefem++ program [11]. According to this program, it is assumed that only first-order derivatives of the desired functions of coordinates will be used in the expression describing the formulation of the problem in the weak form. This is associated with the fact that the solution is sought as an expansion into a series in terms of basic functions that belong to the Sobolev first-order space.

Let us initially consider the calculation of the temperature distribution. For this purpose, we write Eqs. (1) as follows:

$$\nabla\left(\kappa_\mathrm{p}\nabla T\right) = 0. \tag{21}$$

Here, $T$ and $\kappa_\mathrm{p}$ are the temperature and thermal conductivity, respectively, of a substance at a considered point, which may be located both in the gas and in this or that particle. Following the traditional approach [12], let us multiply the right- and left-hand sides of Eq. (21) by some test function $w$, which is smooth in each subregion, and use the Green equation for each subregion assuming that the desired distribution is also described by a smooth function inside of each subregion. As a result, taking into account the properties of the basic functions used for the extrapolation of the desired distribution, we obtain the following [12]:

$$\int_{\Omega} \kappa_{\mathrm{p}} (\nabla T)(\nabla w)\, dV = \int_{\partial\Omega} (\kappa_{\mathrm{p}} \nabla T)\mathbf{n} w\, dS,$$

where $V$ is the volume of considered region $\Omega$, $\partial\Omega$ is the boundary of the considered region, and $S$ is its area. As has been mentioned above, the distributions of the desired values are searched for as expansions into series in terms of basic functions with unknown coefficients. The test functions are successively substituted into the final expressions to derive a set of equations for calculating these unknown coefficients. According to the traditional approach [12], a desired value distribution preset in some portions of the calculation region boundary is taken into account directly when constructing the set of equations, while the value of the test function in these portions is taken equal to zero. This approach is used in the freefem++ program [11]. Therefore, the $w$ function is equal to zero at the boundaries with preset temperatures, and, hence, the integrand in the right-hand side of the obtained expression is equal to zero as well. Consequently, the right-hand side of this equation is equal to zero and the final weak form is as follows [10]:

$$\int_{\Omega} \kappa_{\mathrm{p}} (\nabla T)(\nabla w)\, dV = 0. \tag{22}$$

Note that the use of the Sobolev functional space for the approximation of the desired solution automatically ensures the continuity of the temperature distribution and, hence, the fulfillment of conditions (4) and (8). This, in turn, together with Eq. (21) provides the fulfillment of conditions (5) and (9).

Let us now consider the calculation of velocity distribution. To obtain a corresponding weak form of the problem concerning the velocity distribution, we pass from Eq. (2) to the expression

$$\nabla \cdot \boldsymbol{\sigma}(\mathbf{u}, p) = 0, \tag{23}$$

which is equivalent to the former, provided that condition (3) is met [13]. Here, $\boldsymbol{\sigma}(\mathbf{u}, p)$ is the viscous stress tensor [14]:

$$\boldsymbol{\sigma}(\mathbf{u}, p) = 2\mu \mathbf{D}(\mathbf{u}) - p\mathbf{I},$$

where $\mathbf{I}$ is the unit tensor and $\mathbf{D}(\mathbf{u})$ is the deformation rate tensor,

$$\mathbf{D}(\mathbf{u}) = \frac{1}{2}\left(\nabla \otimes \mathbf{u} + (\nabla \otimes \mathbf{u})^{\mathrm{T}}\right).$$

Multiplying Eqs. (23) and (3) by vector $\mathbf{v}$ and scalar $q$ test functions, respectively; integrating over the considered region; and carrying out a number of transformations [14], we derive the following:

$$\int_{\partial\Omega} (\boldsymbol{\sigma}(\mathbf{u}, p) \cdot \mathbf{n}) \cdot \mathbf{v}\, dS - 2\mu \int_{\Omega} \mathbf{D}(\mathbf{u}) : \mathbf{D}(\mathbf{v})\, dV + \int_{\Omega} p \nabla \cdot \mathbf{v}\, dV + \int_{\Omega} q \nabla \cdot \mathbf{u}\, dV = 0.$$

By specifying the values of $\boldsymbol{\sigma}(\mathbf{u}, p)$ in a portion of the calculation region boundary, we may ensure the uniqueness of the solution of this equation for the velocity field, provided that the velocity has been unambiguously specified for the rest of the boundary [14]. The integration over the portions in which the velocity has been preset is not performed, because the value of the test function in such portions is taken to be zero (see above). As has been mentioned above, components $\boldsymbol{\sigma}(\mathbf{u}, p)$ are equal to zero in all other portions. Therefore, the first term in the last equation may be omitted; as a result, we arrive at the following final weak form:

$$-2\mu \int_{\Omega} \mathbf{D}(\mathbf{u}) : \mathbf{D}(\mathbf{v})\, dV + \int_{\Omega} p \nabla \cdot \mathbf{v}\, dV + \int_{\Omega} q \nabla \cdot \mathbf{u}\, dV = 0. \tag{24}$$

Remember that, in this equation, $\mu$, $\mathbf{u}$, and $p$ are, respectively, the viscosity, velocity, and pressure of the gas or the pseudogas at the point under consideration.

## CALCULATION OF THERMOPHORESIS VELOCITIES FOR SPHERICAL AND SPHEROIDAL PARTICLES

Let us employ the developed scheme for calculating the thermophoresis velocities of axially symmetric particles moving along their common symmetry axis. As a specific example, we consider the motion of a spherical particle, which is referred to as the first one, and a spheroidal particle, which is denoted as the second one, along their common symmetry axis. A constant gas temperature gradient $(\nabla T_{\mathrm{e}})_{\infty}$ directed along the symmetry axis is preset at a large distance from the particles. Since, according to the finite element method, the calculations are always carried out within a finite region, the boundaries of this region are supposed to be located rather far from the particles, while the specification of the temperature gradient at infinity is simulated by presetting a corresponding temperature distribution at these boundaries. If the desired distributions are axially symmetric, which is the case, the requirements to computational resources may be decreased many times by passing to cylindrical coordinates, with this passage reducing the three-dimensional problem to the two-dimensional one, in which all distributions depend only on polar radius $r$

and applicate $z$ of the cylindrical coordinate system. The data necessary for the passage to the cylindrical coordinate system are available from [12] and the manual for the freefem++ program.

Let us now consider the construction of the computational grid and the procedure of the calculation involving the grid. To be more specific, we shall suggest the second particle to have the shape of a flattened spheroid. The structure of the initial calculation region is shown for this case in Fig. 1. To make the representation of individual elements more convenient, the relations between their sizes differ from real ones. Let symbol $a$ denote the distance from the center of the second particle to its surface along the $z$ axis, while symbol $b$ reflects the distance from the center of this particle to its surface in the direction perpendicular to this axis. The latter distance was taken as the radius of the first particle. When constructing the computational grid, distance $b$ was taken as unity. At $a \le b$, the distances from the center of the first particle to the left-hand boundary of the calculation region, from the center of the second particle to the right-hand boundary, and from the $z$ axis to the upper boundary were supposed to be $25b$; in the opposite case, they were taken to be $25a$. The calculations showed that a further increase in the sizes of the considered region had almost no effect on the results obtained. The region under consideration was divided into subregions using the Delone–Voronoi algorithm [16]. The freefem++ program performs this division automatically in accordance with the number of points preset at the boundaries. The temperature distribution over the *ABCD* boundary (Fig. 1) of the calculation region in the gas was assumed to be equal to $T_{01} + z(\nabla T_{\mathrm{e}})_\infty$. The velocity distribution described by Eq. (20) was preset at the calculation region boundary corresponding to the surface of the first particle, and the distribution at the boundary corresponding to the surface of the second particle was determined by an analogous equation. Let us pay attention to the fact that no explicit conditions are imposed on the *AOD* boundary, which coincides with the symmetry axis. As follows from the derivation of expressions (22) and (24), this indicates the existence of implicit boundary conditions, which mean the impermeability of this boundary for the heat fluxes and gas flows. The viscosity of the pseudogas was supposed to be $10^6$ times higher than the viscosity of the gas. At this viscosity of the pseudogas, its velocities at different points appear to be the same within the error of the freefem++ program. The calculations yielded the values of $U_1$ and $U_2$:

$$U_1 = \frac{(U_{\mathrm{T1}})_z}{(U_{\mathrm{TP}})_z},$$

$$U_2 = \frac{g_1}{g_2}\frac{(U_{\mathrm{T2}})_z}{(U_{\mathrm{TP}})_z}.$$

Here, subscript $z$ denotes the projection of a corresponding vector onto the $z$ axis, while $\mathbf{U}_{\mathrm{TP}}$ is the thermophoresis velocity of a solid spherical aerosol particle in an infinite medium [15],

$$\mathbf{U}_{\mathrm{TP}} = -g_1 \frac{2\kappa_{\mathrm{e}}}{\kappa_{\mathrm{i1}} + 2\kappa_{\mathrm{e}}} (\nabla T_{\mathrm{e}})_\infty .$$

The following accuracy criteria were used in the calculations [10]:

$$\varepsilon_1 < \frac{\int_{\Gamma_1} \left( \frac{\mathbf{u\tau}}{g_1} - \boldsymbol{\tau}\nabla T_{\mathrm{e}} \right) dS}{\int_{\Gamma_{\mathrm{i}}} \boldsymbol{\tau}\nabla T_{\mathrm{e}} dS},$$

$$\varepsilon_2 < \frac{\int_{\Gamma_2} \left( \frac{\mathbf{u\tau}}{g_2} - \boldsymbol{\tau}\nabla T_{\mathrm{e}} \right) dS}{\int_{\Gamma_{\mathrm{s}}} \boldsymbol{\tau}\nabla T_{\mathrm{e}} dS}.$$

Here, $\Gamma_1$ and $\Gamma_2$ are the boundaries coinciding with the surfaces of the first and second particles, respectively; $S$ is the length of the boundary that corresponds to the surface of a particle; $\varepsilon_1$ is the relative error in the calculations of $\mathbf{U}_{11}$ and $\mathbf{U}_{21}$; and $\varepsilon_2$ is the relative error in the calculations of $\mathbf{U}_{22}$ and $\mathbf{U}_{12}$. In addition, the accuracy at different elements of the calculation region boundary was controlled by varying the number of points, on the basis of which this region was divided into the subregions. As a result, the number of the subregions for the initial region varied from 28 × $10^3$ to 56 × $10^3$. The maximum possible number of the subregions was determined by the capacity of the RAM available for the calculation; in our case, this size was four gigabyte. This memory capacity was sufficient for calculating the particle velocities with an accuracy of three significant digits. The time of one calculation with the use of an Intel® Core® i3-210 processor was as long as 1.5 min. Basic functions derived from the third-order Legendre polynomials were used to approximate the desired temperature distribution. For the maximum number of subregions, the total number of the degrees of freedom for the space of finite elements was, in this case, as large as 25 × $10^4$. The velocity and pressure fields were approximated using the Legendre polynomials of the third and second orders, respectively. Moreover, as was done in [10], the left-hand side of weak-form equation (23) was supplemented with an additional stabilizing term [12],

$$\varepsilon \int_{\Omega} q p dV,$$

which is in fact the condition of vanishing the average value of the pressure. Here, $\varepsilon$ is a positive small parameter. It may be selected using the following simple approach: if, upon a decrease in a selected value of $\varepsilon$ by several orders of magnitude, the velocity calculated via

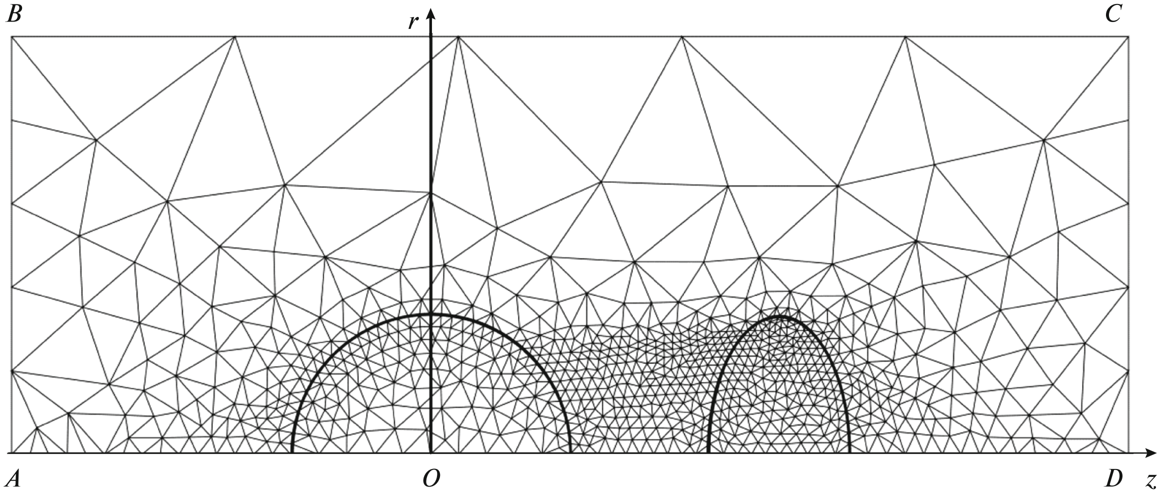

**Fig. 1.** The structure of the initial calculation region.

this algorithm remains unchanged, the selected $^1\varepsilon$ value can be used for the calculation. In our case, this value was taken equal to $10^{-10}$. In all cases, the derived sets of equations with unknown coefficients in the expansions in terms of the basic functions were solved using the UMFPACK iteration algorithm supported by the freefem++ program [17].

The tables presented below list the values of $U_1$ and $U_2$ for different $a/b$ ratios. The accuracy of the presented results does not exceed the accuracy, at which they were obtained according to the aforementioned accuracy criteria. Table 1 shows the $U_1$ and $U_2$ values calculated for two spherical particles. Within the attained accuracy, the presented data coincide with the results of work [6], in which these velocities were

**Table 1.** Normalized thermophoresis velocities of spherical particles

| $h/b$ | $U_1$ | $U_2$ |
|---|---|---|
| $\frac{\kappa_{i1}}{\kappa_e} = \frac{\kappa_{i2}}{\kappa_e} = 10$ | | |
| 0.1 | 1.20 | 1.20 |
| 1 | 1.08 | 1.08 |
| 2 | 1.04 | 1.04 |
| $\frac{\kappa_{i1}}{\kappa_e} = 10, \frac{\kappa_{i2}}{\kappa_e} = 100$ | | |
| 0.1 | 1.28 | 0.105 |
| 1 | 1.07 | 0.148 |
| 2 | 1.03 | 0.134 |
| $\frac{\kappa_{i1}}{\kappa_e} = \frac{\kappa_{i2}}{\kappa_e} = 100$ | | |
| 0.1 | 1.27 | 1.27 |
| 1 | 1.10 | 1.10 |
| 2 | 1.04 | 1.04 |

**Table 2.** Normalized thermophoresis velocities of particles having the shapes of a sphere ($U_1$) and a spheroid with $\frac{a}{b} = 2\,(U_2)$

| $h/b$ | $U_1$ | $U_2$ |
|---|---|---|
| $\frac{\kappa_{i1}}{\kappa_e} = \frac{\kappa_{i2}}{\kappa_e} = 10$ | | |
| 0.1 | 1.18 | 2.03 |
| 1 | 1.14 | 2.01 |
| 2 | 1.07 | 1.97 |
| $\frac{\kappa_{i1}}{\kappa_e} = 10, \frac{\kappa_{i2}}{\kappa_e} = 100$ | | |
| 0.1 | 1.65 | 0.120 |
| 1 | 1.15 | 0.288 |
| 2 | 1.07 | 0.283 |
| $\frac{\kappa_{i1}}{\kappa_e} = 100, \frac{\kappa_{i2}}{\kappa_e} = 10$ | | |
| 0.1 | 0.831 | 19.4 |
| 1 | 1.45 | 17.2 |
| 2 | 1.25 | 16.8 |
| $\frac{\kappa_{i1}}{\kappa_e} = \frac{\kappa_{i2}}{\kappa_e} = 100$ | | |
| 0.1 | 1.60 | 2.64 |
| 1 | 1.20 | 2.43 |
| 2 | 1.10 | 2.37 |

**Table 3.** Normalized thermophoresis velocities of particles having the shapes of a sphere ($U_1$) and a spheroid with $\frac{a}{b} = \frac{1}{2}$ ($U_2$)

| $h/b$ | $U_1$ | $U_2$ |
|---|---|---|
| $\frac{\kappa_{i1}}{\kappa_e} = \frac{\kappa_{i2}}{\kappa_e} = 10$ | | |
| 0.1 | 0.997 | 0.758 |
| 1 | 1.03 | 0.573 |
| 2 | 1.02 | 0.528 |
| $\frac{\kappa_{i1}}{\kappa_e} = 10, \frac{\kappa_{i2}}{\kappa_e} = 100$ | | |
| 0.1 | 1.08 | 0.182 |
| 1 | 1.03 | 0.101 |
| 2 | 1.01 | 0.0744 |
| $\frac{\kappa_{i1}}{\kappa_e} = 100, \frac{\kappa_{i2}}{\kappa_e} = 10$ | | |
| 0.1 | 0.282 | 5.94 |
| 1 | 1.08 | 4.63 |
| 2 | 1.06 | 4.38 |
| $\frac{\kappa_{i1}}{\kappa_e} = \frac{\kappa_{i2}}{\kappa_e} = 100$ | | |
| 0.1 | 1.01 | 0.742 |
| 1 | 1.04 | 0.539 |
| 2 | 1.02 | 0.491 |

found analytically at $g_1 = g_2$. Let us pay attention to the fact that, as the distance between the particles increases, $U_1$ tends to unity, as might be expected for this case.

## CONCLUSIONS

An approach has been described that enables one to employ the finite element method for calculating the thermophoresis velocities of two solid aerosol particles with arbitrary shapes taking into account their interference. The numerical comparison of the results of this approach with the data obtained on the basis of a known analytical solution for spherical particles has indicated that the proposed approach is applicable for the numerical analysis of the thermophoretic motion of two particles, the sizes of which are much larger than the mean free path of molecules in a gas.

## REFERENCES

1. Green, H.L. and Lane, W.R., *Particulate Clouds, Dusts, Smokes, and Mists*, London: Spon, 1957.
2. Reed, L.D. and Morrison, F.A., *J. Aerosol Sci.*, 1975, vol. 6, p. 349.
3. Chen, S.H. and Keh, H.J., *J. Aerosol Sci.*, 1995, vol. 26, p. 429.
4. Yalamov, Yu.I., Gaidukov, M.N., and Levin, V.V., *Teplofiz. Vys. Temp.*, 1994, vol. 32, p. 105.
5. Keh, H.J. and Chen, S.H., *Chem. Eng. Sci.*, 1995, vol. 50, p. 3395.
6. Grashchenkov, S.I., *Cand. Sci. (Phys.-Math.) Dissertation*, Moscow: Ordzhonikidze Moscow Aviation Inst., 1990.
7. Yalamov, Yu.I., Gaidukov, M.N., and Melekhov, A.P., *Dokl. Akad. Nauk SSSR*, 1986, vol. 287, p. 337.
8. Yalamov, Yu.I. and Galoyan, V.S., *Dinamika kapel' v neodnorodnykh vyazkikh sredakh* (Drop Dynamics in Heterogeneous Viscous Media), Yerevan: Luis, 1985.
9. Williams, M.M.R. and Loyalka, S.K., *Aerosol Science: Theory and Practice*, Oxford: Pergamon, 1991.
10. Grashchenkov, S.I., *Colloid J.*, 2017, vol. 79, p. 35.
11. Hecht, F., *J. Num. Math.*, 2012, vol. 20, p. 251.
12. Reddy, J.N. and Gartling, D.K., *The Finite Element Method in Heat Transfer and Fluid Dynamics*, Boca Raton: CRC, 2010.
13. Pozrikidis, C., *Introduction to Theoretical and Computational Fluid Dynamics*, Oxford: Oxford Univ. Press, 2011.
14. Glowinski, R., in *Handbook of Numerical Analysis*, 2003, vol. 9, p. 3.
15. Epstein, P.S., *Z. Phys.*, 1929, vol. 54, p. 537.
16. Lucquin, B. and Pironneau, O., *Introduction to Scientific Computing*, Chichester: Wiley, 1998.
17. Davis, T.A., *ACM Trans. Math. Software*, 2004, vol. 30, p. 196.

*Translated by A. Kirilin*